

Review

A study of reaction wheel configurations for a 3-axis satellite attitude control

Zuliana Ismail *, Renuganth Varatharajoo

Department of Aerospace Engineering, Faculty of Engineering, University Putra Malaysia, 43400 Selangor, Malaysia

Received 16 September 2008; received in revised form 27 October 2009; accepted 10 November 2009

Abstract

The satellite reaction wheel's configuration plays also an important role in providing the attitude control torques. Several configurations based on three or four reaction wheels are investigated in order to identify the most suitable orientation that consumes a minimum power. Such information in a coherent form is not summarized in any publication; and therefore, an extensive literature search is required to obtain these results. In addition, most of the available results are from different test conditions; hence, making them difficult for comparison purposes. In this work, the standard reaction wheel control and angular momentum unloading schemes are adopted for all the reaction wheel configurations. The schemes will be presented together with their governing equations, making them fully amenable to numerical treatments. Numerical simulations are then performed for all the possible reaction wheel configurations with respect to an identical reference mission. All the configurations are analyzed in terms of their torques, momentums and attitude control performances. Based on the simulations, the reaction wheel configuration that has a minimum total control torque level is identified, which also corresponds to the configuration with minimum power consumption.

© 2009 COSPAR. Published by Elsevier Ltd. All rights reserved.

Keywords: Reaction wheel; Satellite attitude control; Momentum management

Contents

1. Introduction	751
2. Reaction wheel control structure	751
2.1. Attitude dynamics and kinematics	751
2.2. Reaction wheel momentum unloading	753
2.3. Reaction wheel control strategy	755
3. Attitude control performances	758
4. Summarization	758
5. Wheel angular momentum control performance	759
6. Conclusion	759
References	759

* Corresponding author. Tel.: +60 38 9466406; fax: +60 38 6567125.

E-mail addresses: zuliana.ismail@gmail.com (Z. Ismail), renu99@gmx.de (R. Varatharajoo).

1. Introduction

Many satellite missions employ gravity gradient stabilization or only magnetic control technique to control the satellite's attitude. These methods have been used because they are simple in nature and require a minimum cost. Unfortunately, they can only provide low pointing accuracies and limited control torques due to their dependability on the gravitational field and the geomagnetic field condition (Chen et al., 2000; Silani and Lovera, 2005). Instead, costly but effective actuator named reaction wheels have been extensively used for satellite attitude control both for large satellites (Beals et al., 1988; Radford et al., 1996) and small satellites (Zee et al., 2002; Brieß et al., 2005). Almost all satellite missions with reaction wheels as attitude actuators proved that a high attitude control performance can be achieved and satisfy the mission requirements.

It is common to equip the satellite with three reaction wheels for a 3-axis control (Kim et al., 1996; Nudehi et al., 2008). However, having four reaction wheels is the best option for redundancy reasons (Won, 1999; Wisniewski and Kulczycki, 2005; Jin et al., 2008). This is because if one of the reaction wheels fails, the satellite can still be controlled by the remaining three wheels or even if two of the reaction wheels fail, there are still two reaction wheels left to control the satellite's attitude (Krishnan et al., 1995; Urakubo et al., 2004). In fact, several researches focused on the attitude control of a satellite with only two reaction wheels (Ge and Chen, 2004; Boyer and Alami, 2007). Another factor to be considered is the reaction wheel saturation due to the constant external disturbance torques (Bang et al., 2003). Thus, it is compulsory for a satellite to be equipped with a momentum management scheme in order to remove its excess wheel momentum (Burns and Flashner, 1992; Karami and Sassani, 2007). Another external torque source, such as thrusters and magnetic torquers, has been suggested to unload the wheel angular momentum (Oh et al., 1996; Chen et al., 1999). However, magnetic torquers are more preferred as they are cheaper compared to the thrusters that consume large amount of fuel (Johnson and Skelton, 1971; Camillo and Markley, 1980; Giuliatti et al., 2006).

Since the reaction wheel is electrically driven by a motor, power is highly used by the attitude control system that employs reaction wheels. Therefore, the power consumption has to be minimized as much as possible especially for small satellite missions in order to employ multiple reaction wheels on-board the satellite (Grassi and Pastena, 2000). Until now, there are numbers of research regarding the power consumption of the reaction wheel as an attitude control actuator (Zhaowei et al., 2004; Ma et al., 2003; Sinclair et al., 2007). However, their works are focused on the controller and reaction wheel sizing optimization. Basically, the power consumed by the reaction wheels can be lowered by particularly arranging the reaction wheels' orientation on-board the satellite. There are very few researches on this issue (Hablani, 1994; Bayard, 2001). Moreover, the study presented in Hablani (1994) is focused

on a single configuration optimization while the research done by Bayard (2001) is limited to three reaction wheels' configuration.

In contrast, this study summarizes several typical reaction wheel orientations on-board the satellite corresponding to their total control torques needed to maintain a 3-axis attitude control. It is worthwhile to mention that such a study is not performed in a coherent form before; hence, an extensive literature search is needed in order to gather such results. Even then, the available test cases are all different (e.g., mission, controller, etc.); and therefore, making them difficult for comparison purposes. This study is done for two configurations, the first for three reaction wheels and the second for four reaction wheels. In this paper, the standard mathematical models of the satellite attitude control system with reaction wheels are described. The standard algorithms for angular momentum unloading using three magnetic torquers are also presented. The conventional PD-type (proportional-derivative) controller and PI-type (proportional-integral) controller are adopted for the satellite attitude and wheel angular momentum controls, respectively. The suitable reaction wheel orientation that produces a minimum total control torque can be identified by estimating the total torques required to maintain the 3-axis satellite attitude control. In addition, the effectiveness of the standard attitude controller in a various reaction wheel configurations can be also observed.

The paper is organized as follows: the standard satellite attitude dynamics and kinematics equation are formulated in Section 2; the reaction wheel's momentum management and the reaction wheel configurations for a several case studies are also presented in that section; the reference mission is introduced and the attitude control performances for all the test cases are discussed in Section 3; the result summarization is given concisely in Section 4; the wheel angular momentum unloading performance is shown in Section 5 and the conclusion is drawn in Section 6.

2. Reaction wheel control structure

2.1. Attitude dynamics and kinematics

Based on the Euler's equation and Newton's third law, the dynamic equation of a satellite motion with reaction wheels and magnetorquers can be written as (Kim et al., 1996; Won, 1999)

$$\mathbf{I} \cdot \dot{\boldsymbol{\omega}}_{\text{IE/B}} = \mathbf{T}_d + \mathbf{T}_m - \boldsymbol{\omega}_{\text{IE/B}} \times (\mathbf{I} \cdot \boldsymbol{\omega}_{\text{IE/B}} + \mathbf{h}_w) - \mathbf{T}_w \quad (1)$$

where $\mathbf{I} = \text{diag}[I_x \ I_y \ I_z]$ is the moments of inertia of the satellite's body, $\boldsymbol{\omega}_{\text{IE/B}} = [\omega_x \ \omega_y \ \omega_z]^T$ is the inertially referenced satellite angular rate vector of the satellite body relative to the inertial coordinate system, \mathbf{h}_w is the reaction wheel angular momentum vector, \mathbf{T}_w is the applied reaction wheel torques, \mathbf{T}_m is the magnetic torque vector induced by magnetic torquers and \mathbf{T}_d is the external disturbance torques vector. By taking $\mathbf{T}_d + \mathbf{T}_m - \mathbf{T}_w$ as the total torques $\mathbf{T} = [T_x \ T_y \ T_z]^T$ applied on the satellite, the satellite dy-

dynamic equations (roll, yaw and pitch) can be represented as follows

$$\begin{aligned}\dot{\omega}_x &= \frac{T_x - (I_y - I_z)\omega_y\omega_z + h_{wy}\omega_y - h_{wz}\omega_z}{I_x} \\ \dot{\omega}_y &= \frac{T_y - (I_z - I_x)\omega_x\omega_z + h_{wx}\omega_x - h_{wz}\omega_z}{I_y} \\ \dot{\omega}_z &= \frac{T_z - (I_x - I_y)\omega_x\omega_y + h_{wx}\omega_x - h_{wy}\omega_y}{I_z}\end{aligned}\quad (2)$$

Quaternion is used for the attitude representation herein. Therefore, the derivatives of the Euler parameters can be updated by using the kinematics equation as follows (Sidi, 1997)

$$\dot{\mathbf{q}} = \frac{1}{2}\Omega(\omega_{IE/B}) \cdot \mathbf{q} \quad (3)$$

where \mathbf{q} is an attitude quaternion that represents the attitude of the satellite relative to the local-vertical-local-hor-

izontal (LVLH) coordinate system and $\Omega(\omega_{IE/B})$ is the skew symmetric matrix.

The command control torques \mathbf{T}_a is related to the quaternion and angular rate errors. The standard PD-type controller is employed for the 3-axis attitude control (Won, 1999). The control law can be represented as

$$\mathbf{T}_a = -2\mathbf{K}_p\mathbf{q}_e - \mathbf{K}_d\omega_e \quad (4)$$

where the error quaternion \mathbf{q}_e is the quaternion difference between the commanded quaternion \mathbf{q}_{cmd} and the current quaternion \mathbf{q}_c . Whereas, ω_e is the angular rate difference between the commanded angular rate ω_{cmd} and the current angular rate ω_c .

In order to generate sufficient control torques from the control law, the proportional gain $K_p = \omega_n^2 I$ and derivative gain $K_d = 2\xi\omega_n I$ are to be chosen accordingly. These control gains are the functions of dynamic characteristics, i.e., the natural frequency ω_n and the damping ratio ξ .

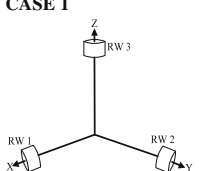
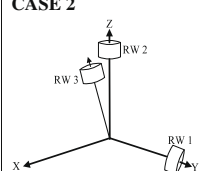
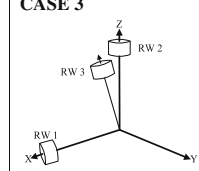
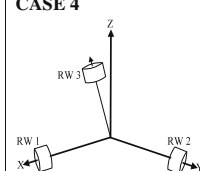
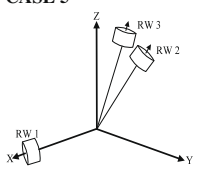
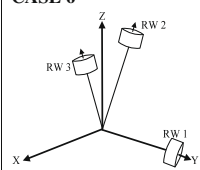
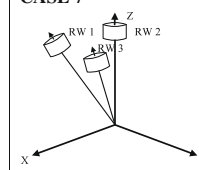
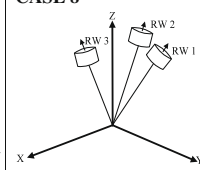
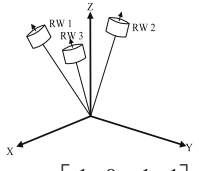
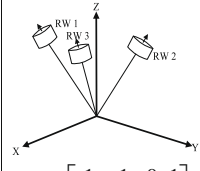
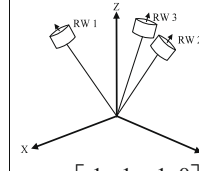
<p>CASE 1</p>  $A_w = \begin{bmatrix} 1 & 0 & 0 & 0 \\ 0 & 1 & 0 & 0 \\ 0 & 0 & 1 & 0 \end{bmatrix}$	<p>CASE 2</p>  $A_w = \begin{bmatrix} 0 & 0 & 0 & 1 \\ 0 & 1 & 0 & 1 \\ 0 & 0 & 1 & 1 \end{bmatrix}$ <p>-RW 3 tilted on (x, y) plane.</p>	<p>CASE 3</p>  $A_w = \begin{bmatrix} 1 & 0 & 0 & 1 \\ 0 & 0 & 0 & 1 \\ 0 & 0 & 1 & 1 \end{bmatrix}$ <p>-RW 3 tilted on (x, y) plane.</p>	<p>CASE 4</p>  $A_w = \begin{bmatrix} 1 & 0 & 0 & 1 \\ 0 & 1 & 0 & 1 \\ 0 & 0 & 0 & 1 \end{bmatrix}$ <p>-RW 3 tilted on (x, y) plane.</p>
<p>CASE 5</p>  $A_w = \begin{bmatrix} 1 & -1 & -1 & 0 \\ 0 & 1 & -1 & 0 \\ 0 & 1 & 1 & 0 \end{bmatrix}$ <p>-RW 2 tilted on (-x, y) plane. -RW 3 tilted on (-x, y) plane.</p>	<p>CASE 6</p>  $A_w = \begin{bmatrix} 0 & 0 & -1 & 1 \\ 0 & 1 & -1 & 1 \\ 0 & 0 & 1 & 1 \end{bmatrix}$ <p>-RW 2 tilted on (-x, -y) plane. -RW 3 tilted on (x, y) plane.</p>	<p>CASE 7</p>  $A_w = \begin{bmatrix} 1 & 0 & 0 & 1 \\ -1 & 0 & 0 & 1 \\ 1 & 0 & 1 & 1 \end{bmatrix}$ <p>-RW 1 tilted on (x, -y) plane. -RW 3 tilted on (x, y) plane.</p>	<p>CASE 8</p>  $A_w = \begin{bmatrix} 0 & -1 & -1 & 1 \\ 0 & 1 & -1 & 1 \\ 0 & 1 & 1 & 1 \end{bmatrix}$ <p>-RW 1 tilted on (-x, y) plane. -RW 2 tilted on (-x, -y) plane. -RW 3 tilted on (x, y) plane.</p>
<p>CASE 9</p>  $A_w = \begin{bmatrix} 1 & 0 & -1 & 1 \\ -1 & 0 & -1 & 1 \\ 1 & 0 & 1 & 1 \end{bmatrix}$ <p>-RW 1 tilted on (x, -y) plane. -RW 2 tilted on (-x, -y) plane. -RW 3 tilted on (x, y) plane.</p>	<p>CASE 10</p>  $A_w = \begin{bmatrix} 1 & -1 & 0 & 1 \\ -1 & 1 & 0 & 1 \\ 1 & 1 & 0 & 1 \end{bmatrix}$ <p>-RW 1 tilted on (x, -y) plane. -RW 2 tilted on (-x, y) plane. -RW 3 tilted on (x, y) plane.</p>	<p>CASE 11</p>  $A_w = \begin{bmatrix} 1 & -1 & -1 & 0 \\ -1 & 1 & -1 & 0 \\ 1 & 1 & 1 & 0 \end{bmatrix}$ <p>-RW 1 tilted on (x, -y) plane. -RW 2 tilted on (-x, y) plane. -RW 3 tilted on (-x, -y) plane.</p>	

Fig. 1. Configuration matrix of three reaction wheels.

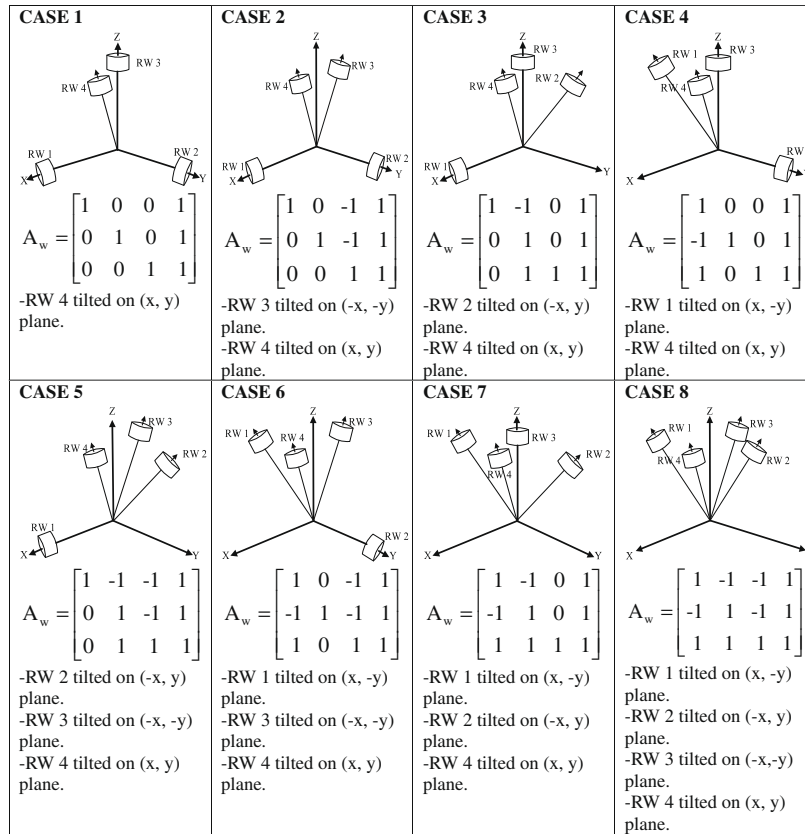


Fig. 2. Configuration matrix of four reaction wheels.

In addition, the derivation of Euler angles (roll (R), pitch (P) and yaw (Y)) error $[\phi, \theta, \psi]^T$ from the attitude quaternion error is as follows (Sidi, 1997)

$$\begin{bmatrix} \phi \\ \theta \\ \psi \end{bmatrix} = \begin{bmatrix} \arctan\left(\frac{2(q_1q_4 + q_2q_3)}{1 - 2(q_1^2 + q_2^2)}\right) \\ \arcsin(2(q_4q_2 - q_3q_1)) \\ \arctan\left(\frac{2(q_4q_3 + q_1q_2)}{1 - 2(q_2^2 + q_3^2)}\right) \end{bmatrix} \quad (5)$$

2.2. Reaction wheel momentum unloading

Reaction wheel angular momentum tends to constantly increase or decrease in the presence of constant external disturbances; hence, it induces a build-up in the wheel momentum. The external torque by magnetorquers is desirable here to dump the wheel momentum to its original level. The unloading control law should be implemented in order to control the amount of the required magnetic torques to be exerted by the magnetic torquers (Bang et al., 2003; Chen et al., 1999).

The control magnetic dipole moment \mathbf{m} can be calculated using the wheel unloading law defined as (Camillo and Markley, 1980; Burns and Flashner, 1992; Oh et al., 1996)

$$\mathbf{m} = -\frac{k}{B^2}(\mathbf{b} \times \Delta\mathbf{h}) \quad (6)$$

where k is the unloading control gain, \mathbf{b} is the Earth's magnetic field, $\Delta\mathbf{h} = \mathbf{h}_{wc} - \mathbf{h}_w$ is the angular momentum system error, \mathbf{h}_{wc} is the wheel's current momentum vector and \mathbf{h}_w is the wheel's previous momentum vector.

The wheel unloading control is based on the PI-type controller and the transfer function of the momentum unloading system is

$$\frac{h_{wc}}{h_{wo}}(s) = \frac{K_P s + K_I}{s^2 + K_P s + K_I} \quad (7)$$

where $K_P = 2\zeta\omega_n$ and $K_I = \omega_n^2$ are the proportional and integral gains, respectively.

On the other hand, a simple dipole model is used to calculate the Earth's magnetic field \mathbf{b} in the LVLH coordinate system, the vector \mathbf{b} that is a function of time can be expressed as (Steyn, 1994; Psiaki, 2001; Giulietti et al., 2006)

$$\begin{bmatrix} b_x(t) \\ b_y(t) \\ b_z(t) \end{bmatrix} = \begin{bmatrix} B_x \cdot \cos(\omega_o t) \\ B_y \\ B_z \cdot \sin(\omega_o t) \end{bmatrix} \quad (8)$$

Table 1
Reference orbit parameters.

Inclination, i	83 deg
Altitude, h	470 km
Right ascension, Ω	15.7 deg
Period, t	5640 s (1 orbit)
Orbital frequency, ω_o	0.0011 rad/s

Table 2

Reference satellite specifications.

Moments of inertia matrix	$\mathbf{I} = \begin{bmatrix} 4.2 & 0 & 0 \\ 0 & 4.4 & 0 \\ 0 & 0 & 4.2 \end{bmatrix} \text{ kg m}^2$
Attitude control gains	$K_{px} = 0.672 \text{ N m/rad}$, $K_{py} = 0.704 \text{ Nm/rad}$, $K_{pz} = 0.672 \text{ Nm/rad}$ $K_{dx} = 3.36 \text{ N m s/rad}$, $K_{dy} = 3.52 \text{ N m s/rad}$, $K_{dz} = 3.36 \text{ N m s/rad}$
Unloading control gains	$K_{px} = 0.00136 \text{ rad/s}$, $K_{py} = 0.00069 \text{ rad/s}$, $K_{pz} = 0.00094 \text{ rad/s}$ $K_{ix} = 4.624 \times 10^{-7} \text{ rad}^2/\text{s}^2$, $K_{iy} = 1.19 \times 10^{-7} \text{ rad}^2/\text{s}^2$ $K_{iz} = 2.21 \times 10^{-7} \text{ rad}^2/\text{s}^2$
Limit of the reaction wheel torques	$\mathbf{T}_c = [0.1 \quad 0.1 \quad 0.1 \quad 0.1]^T \text{ N m}$
Saturation limit of magnetic torquers	$\mathbf{m} = \pm 12 \text{ A m}^2$
External disturbance torques	$\begin{bmatrix} T_{dx} \\ T_{dy} \\ T_{dz} \end{bmatrix} = \begin{bmatrix} 8 \times 10^{-5} \sin(\omega_o t) \\ 8 \times 10^{-6} + 8 \times 10^{-5} \sin(\omega_o t) + 5 \times 10^{-5} \cos(\omega_o t) \\ 8 \times 10^{-6} + 5 \times 10^{-5} \cos(\omega_o t) \end{bmatrix} \text{ N m}$
Initial attitude errors	$[\phi, \theta, \psi] = \pm 5 \text{ deg}$

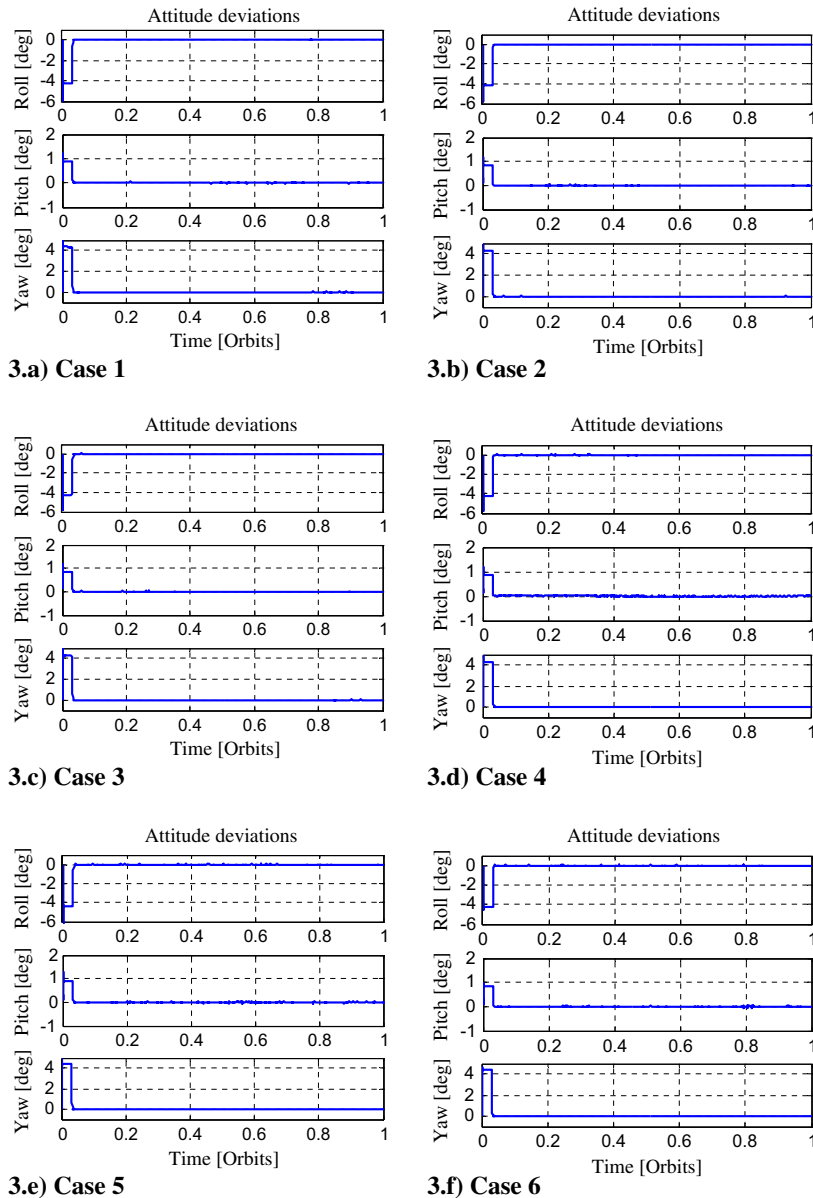


Fig. 3. Performances of three reaction wheels.

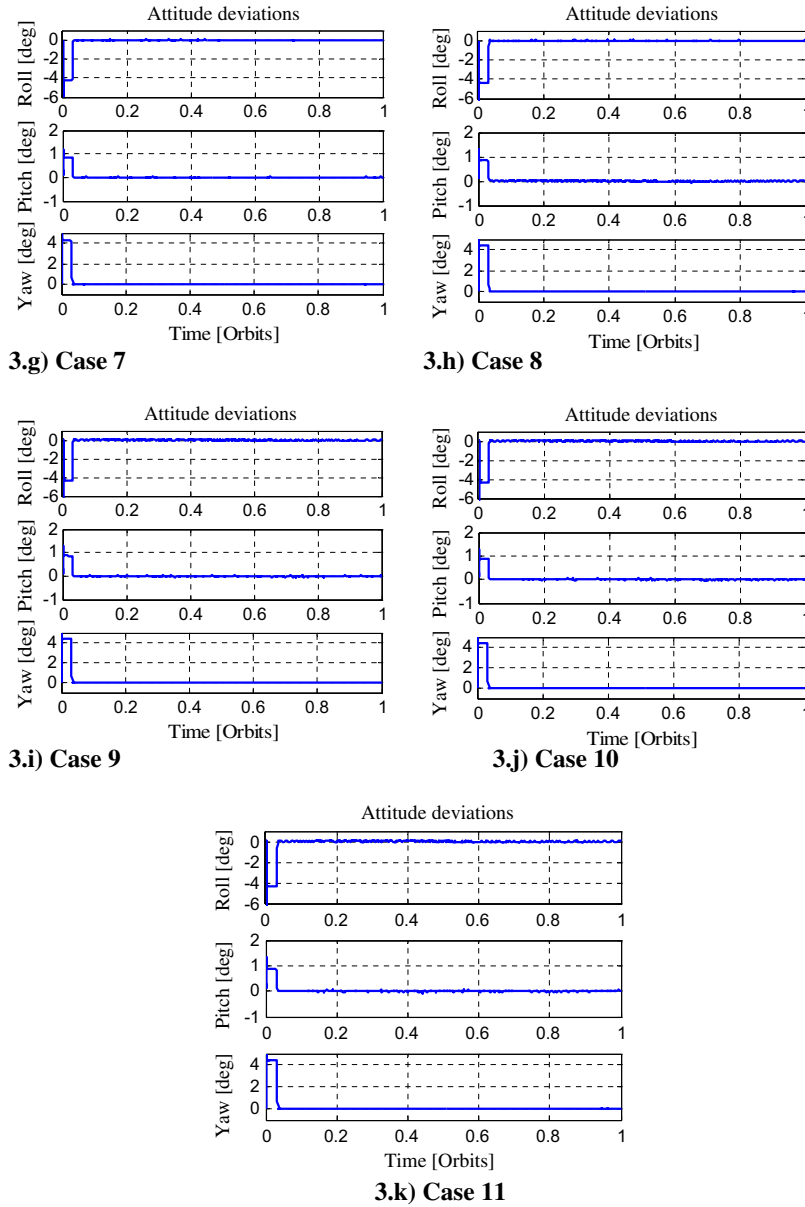


Fig. 3 (continued)

where ω_o is the orbit rotation frequency and t is the time measured from $t = 0$ at the ascending node crossing of the magnetic equator. Whereas the magnitude of B_x , B_y , B_z is the function of the orbit inclination and can be written as

$$\begin{bmatrix} B_x \\ B_y \\ B_z \end{bmatrix} = \begin{bmatrix} -B_o \sin(i) \\ B_o \cos(i) \\ -2B_o \sin(i) \end{bmatrix} \quad (9)$$

where B_o is the average magnetic field intensity in a low earth orbit ($B_o = 2 \times 10^{-5}$ [Tesla]) and i is the orbit inclination with respect to the magnetic equator. Once the control magnetic dipole moment \mathbf{m} has been estimated according to Eq. (6), the magnetic control torque vector \mathbf{T}_m can be calculated as follows (Burns and Flashner, 1992; Sidi, 1997)

$$\mathbf{T}_m = \mathbf{m} \times \mathbf{B} \quad (10)$$

where \mathbf{B} is the Earth's magnetic field in the satellite body coordinate system.

2.3. Reaction wheel control strategy

Consider that four reaction wheels are installed onboard the satellite and denote the \mathbf{T}_c as the wheel control torque, the applied 3-axis control torque \mathbf{T}_w from the reaction wheels can be calculated as (Tavakkoli et al., 2005)

$$\begin{bmatrix} T_{wx} \\ T_{wy} \\ T_{wz} \end{bmatrix} = [A_w] \cdot \begin{bmatrix} T_{c1} \\ T_{c2} \\ T_{c3} \\ T_{c4} \end{bmatrix} \quad (11)$$

where A_w is the reaction wheel configuration matrix defined as

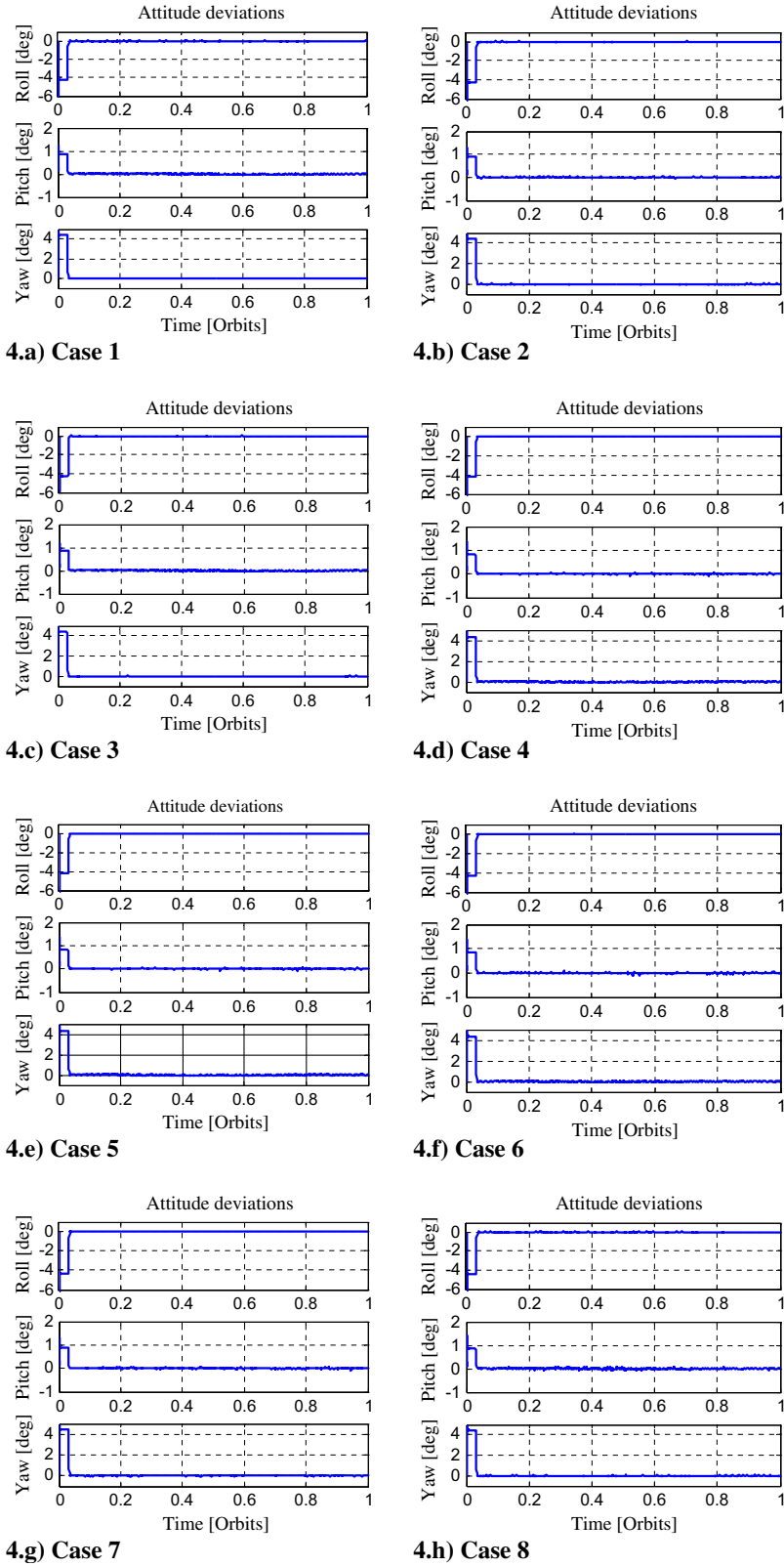


Fig. 4. Performances of four reaction wheels.

$$A_w = [a_{1,w} \ a_{2,w} \ a_{3,w} \ a_{4,w}] \quad (12)$$

whereby $\mathbf{a}_{i,w}$ is the unit vector in the direction of the spin axis of the i th reaction wheel. Assume that if there are three

reaction wheels aligned on the primary axis of the satellite and a redundant wheel tilted at an equal angle from the others, A_w can be defined as

$$A_w = \begin{bmatrix} 1 & 0 & 0 & 1 \\ 0 & 1 & 0 & 1 \\ 0 & 0 & 1 & 1 \end{bmatrix} \quad (13)$$

Matrix A_w only shows the influence of the reaction wheel to a particular axis. Note that in the case of tilted reaction wheels, the induced torque on the satellite body depends on the tilted angle as well, i.e., $T_c \cos 45^\circ$ or $T_c \sin 45^\circ$ in this work.

The pseudo-inverse of the reaction wheel configuration matrix A_w^{-1} can be multiplied with the commanded control torques T_a obtained in Eq. (4) in order to determine the magnitudes of T_c as follows

$$\begin{bmatrix} T_{c1} \\ T_{c2} \\ T_{c3} \\ T_{c4} \end{bmatrix} = [A_w^{-1}] \cdot \begin{bmatrix} T_{ax} \\ T_{ay} \\ T_{az} \end{bmatrix} \quad (14)$$

The configuration matrix in Eq. (13) is representing just one of the possible reaction wheel orientations that can be implemented on-board a satellite. Actually, there are more

possible orientations available without degrading the 3-axis attitude control. The different configurations that are proposed in this study for three reaction wheels and four reaction wheels are summarized in Figs. 1 and 2, respectively. Among those configurations, the suitable reaction wheel orientation that consumes a minimum current can be identified by calculating their total minimum torques required to maintain the 3-axis satellite attitude control.

Table 3
Performance analysis of three reaction wheels.

Case	Reaction wheel torques [N m]	Wheel angular momentums [N m s]	Attitude errors [deg]
Case 1	$ T_{wx} _{\max} = 3.3 \times 10^{-6}$ $ T_{wy} _{\max} = 1.3 \times 10^{-5}$ $ T_{wz} _{\max} = 9.3 \times 10^{-6}$ $T_{w_total} = 2.56 \times 10^{-5}$	$ h_{wx} _{\max} = 0.0665$ $ h_{wy} _{\max} = 0.0994$ $ h_{wz} _{\max} = 0.0128$ $h_{w_total} = 0.179$	$ \phi _{\max} = 0.0002$ $ \theta _{\max} = 0.0001$ $ \psi _{\max} = 0.0001$ Total < 0.001
Case 2	$ T_{wx} _{\max} = 5.6 \times 10^{-6}$ $ T_{wy} _{\max} = 5.4 \times 10^{-6}$ $ T_{wz} _{\max} = 7.0 \times 10^{-6}$ $T_{w_total} = 1.80 \times 10^{-5}$	$ h_{wx} _{\max} = 0.0667$ $ h_{wy} _{\max} = 0.0996$ $ h_{wz} _{\max} = 0.0128$ $h_{w_total} = 0.179$	$ \phi _{\max} = 0.0003$ $ \theta _{\max} = 0.0004$ $ \psi _{\max} = 0.0004$ Total ≈ 0.001
Case 3	$ T_{wx} _{\max} = 2.5 \times 10^{-8}$ $ T_{wy} _{\max} = 6.5 \times 10^{-6}$ $ T_{wz} _{\max} = 8.4 \times 10^{-6}$ $T_{w_total} = 1.49 \times 10^{-5}$	$ h_{wx} _{\max} = 0.0667$ $ h_{wy} _{\max} = 0.0996$ $ h_{wz} _{\max} = 0.0128$ $h_{w_total} = 0.179$	$ \phi _{\max} = 0.0001$ $ \theta _{\max} = 0.0004$ $ \psi _{\max} = 0.0002$ Total ≈ 0.001
Case 4	$ T_{wx} _{\max} = 3.5 \times 10^{-6}$ $ T_{wy} _{\max} = 5.0 \times 10^{-6}$ $ T_{wz} _{\max} = 9.5 \times 10^{-6}$ $T_{w_total} = 1.80 \times 10^{-5}$	$ h_{wx} _{\max} = 0.0665$ $ h_{wy} _{\max} = 0.0994$ $ h_{wz} _{\max} = 0.0128$ $h_{w_total} = 0.179$	$ \phi _{\max} = 0.0002$ $ \theta _{\max} = 0.0005$ $ \psi _{\max} = 0.0002$ Total ≈ 0.001
Case 5	$ T_{wx} _{\max} = 6.8 \times 10^{-6}$ $ T_{wy} _{\max} = 2.6 \times 10^{-6}$ $ T_{wz} _{\max} = 3.1 \times 10^{-6}$ $T_{w_total} = 1.25 \times 10^{-5}$	$ h_{wx} _{\max} = 0.0665$ $ h_{wy} _{\max} = 0.0994$ $ h_{wz} _{\max} = 0.0128$ $h_{w_total} = 0.179$	$ \phi _{\max} = 0.0001$ $ \theta _{\max} = 0.0004$ $ \psi _{\max} = 0.0009$ Total ≈ 0.001
Case 6	$ T_{wx} _{\max} = 2.6 \times 10^{-6}$ $ T_{wy} _{\max} = 1.1 \times 10^{-5}$ $ T_{wz} _{\max} = 7.2 \times 10^{-6}$ $T_{w_total} = 2.10 \times 10^{-5}$	$ h_{wx} _{\max} = 0.0667$ $ h_{wy} _{\max} = 0.0996$ $ h_{wz} _{\max} = 0.0128$ $h_{w_total} = 0.179$	$ \phi _{\max} = 0.0002$ $ \theta _{\max} = 0.0002$ $ \psi _{\max} = 0.0003$ Total ≈ 0.001
Case 7	$ T_{wx} _{\max} = 1.8 \times 10^{-6}$ $ T_{wy} _{\max} = 5.1 \times 10^{-6}$ $ T_{wz} _{\max} = 1.2 \times 10^{-5}$ $T_{w_total} = 1.89 \times 10^{-5}$	$ h_{wx} _{\max} = 0.0667$ $ h_{wy} _{\max} = 0.0996$ $ h_{wz} _{\max} = 0.0128$ $h_{w_total} = 0.179$	$ \phi _{\max} = 0.0002$ $ \theta _{\max} = 0.0005$ $ \psi _{\max} = 0.0001$ Total ≈ 0.001
Case 8	$ T_{wx} _{\max} = 3.4 \times 10^{-6}$ $ T_{wy} _{\max} = 6.4 \times 10^{-6}$ $ T_{wz} _{\max} = 9.1 \times 10^{-6}$ $T_{w_total} = 1.89 \times 10^{-5}$	$ h_{wx} _{\max} = 0.0666$ $ h_{wy} _{\max} = 0.0994$ $ h_{wz} _{\max} = 0.0128$ $h_{w_total} = 0.179$	$ \phi _{\max} = 0.0001$ $ \theta _{\max} = 0.0003$ $ \psi _{\max} = 0.0010$ Total ≈ 0.001
Case 9	$ T_{wx} _{\max} = 5.20 \times 10^{-6}$ $ T_{wy} _{\max} = 3.10 \times 10^{-6}$ $ T_{wz} _{\max} = 1.96 \times 10^{-5}$ $T_{w_total} = 2.79 \times 10^{-5}$	$ h_{wx} _{\max} = 0.0665$ $ h_{wy} _{\max} = 0.0994$ $ h_{wz} _{\max} = 0.0128$ $h_{w_total} = 0.179$	$ \phi _{\max} = 0.0004$ $ \theta _{\max} = 0.0006$ $ \psi _{\max} = 0.0002$ Total ≈ 0.001
Case 10	$ T_{wx} _{\max} = 6.2 \times 10^{-6}$ $ T_{wy} _{\max} = 9.8 \times 10^{-6}$ $ T_{wz} _{\max} = 2.2 \times 10^{-6}$ $T_{w_total} = 1.82 \times 10^{-5}$	$ h_{wx} _{\max} = 0.0666$ $ h_{wy} _{\max} = 0.0994$ $ h_{wz} _{\max} = 0.0128$ $h_{w_total} = 0.179$	$ \phi _{\max} = 0.0001$ $ \theta _{\max} = 0.0001$ $ \psi _{\max} = 0.0008$ Total ≈ 0.001
Case 11	$ T_{wx} _{\max} = 9.4 \times 10^{-7}$ $ T_{wy} _{\max} = 1.3 \times 10^{-5}$ $ T_{wz} _{\max} = 6.7 \times 10^{-6}$ $T_{w_total} = 2.07 \times 10^{-5}$	$ h_{wx} _{\max} = 0.0666$ $ h_{wy} _{\max} = 0.0993$ $ h_{wz} _{\max} = 0.0128$ $h_{w_total} = 0.179$	$ \phi _{\max} = 0.0002$ $ \theta _{\max} = 0.0003$ $ \psi _{\max} = 0.0002$ Total ≈ 0.001

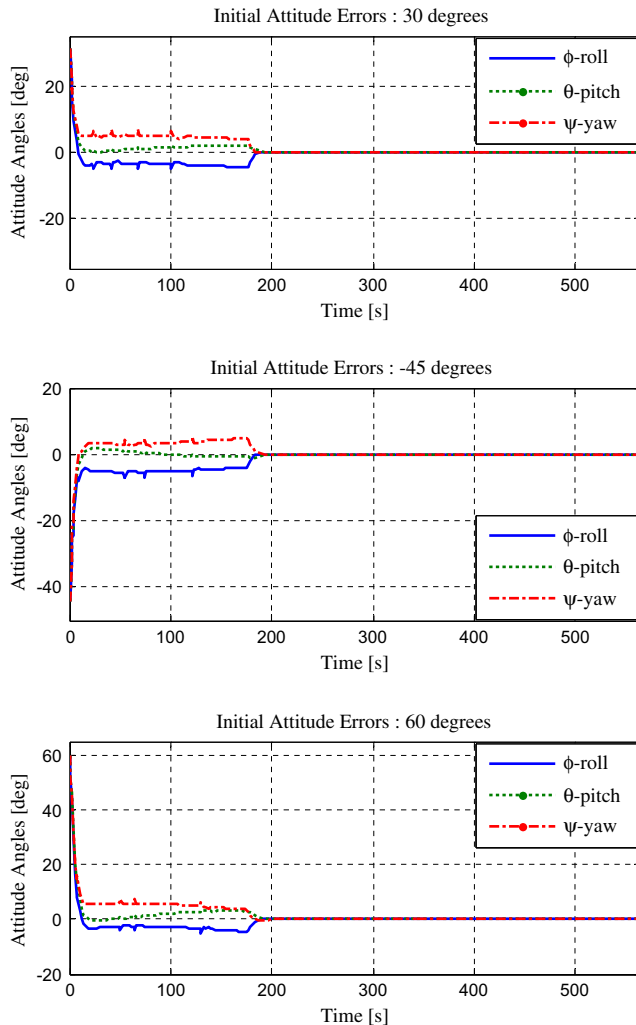


Fig. 5. Attitude performances for different initial attitude errors.

3. Attitude control performances

In order to simulate the satellite attitude control performance, a reference mission is proposed in Tables 1 and 2. All the reaction wheels are assumed to be identical and their configurations will be simulated using the reference mission. The governing equations and the reference mission's parameters are implemented in the Matlab®–Simulink™ codes. Then, numerical treatments are performed, which allow an assessment of each configuration's merits. The simulation result pertaining to each configuration is carefully evaluated in terms of their torques, momentums and attitude control performances. The reaction wheel configuration that has a minimum total control torque level is identified in order to determine a minimum power intake configuration.

Fig. 3a–k represents the satellite attitude control performances for three reaction wheels corresponding to their configurations in Fig. 1. Whereas Fig. 4a–h represents the satellite attitude control performances for four reaction wheels corresponding to their configurations in Fig. 2.

Table 4
Performance analysis of four reaction wheels.

Case	Reaction wheel torques [N m]	Angular momentums [N m s]	Attitude errors [deg]
Case 1	$ T_{wx} _{\max} = 9.1 \times 10^{-6}$ $ T_{wy} _{\max} = 6.9 \times 10^{-7}$ $ T_{wz} _{\max} = 3.7 \times 10^{-6}$ $T_{w_total} = 1.35 \times 10^{-5}$	$ h_{wx} _{\max} = 0.0666$ $ h_{wy} _{\max} = 0.0993$ $ h_{wz} _{\max} = 0.0129$ $h_{w_total} = 0.179$	$ \phi _{\max} = 0.0004$ $ \theta _{\max} = 0.0007$ $ \psi _{\max} = 0.0001$ Total ≈ 0.001
Case 2	$ T_{wx} _{\max} = 3.8 \times 10^{-6}$ $ T_{wy} _{\max} = 6.0 \times 10^{-6}$ $ T_{wz} _{\max} = 2.9 \times 10^{-6}$ $T_{w_total} = 1.27 \times 10^{-5}$	$ h_{wx} _{\max} = 0.0667$ $ h_{wy} _{\max} = 0.0998$ $ h_{wz} _{\max} = 0.0129$ $h_{w_total} = 0.179$	$ \phi _{\max} = 0.0001$ $ \theta _{\max} = 0.0004$ $ \psi _{\max} = 0.0009$ Total ≈ 0.001
Case 3	$ T_{wx} _{\max} = 4.1 \times 10^{-6}$ $ T_{wy} _{\max} = 3.83 \times 10^{-6}$ $ T_{wz} _{\max} = 6.4 \times 10^{-7}$ $T_{w_total} = 8.57 \times 10^{-6}$	$ h_{wx} _{\max} = 0.0666$ $ h_{wy} _{\max} = 0.0995$ $ h_{wz} _{\max} = 0.0128$ $h_{w_total} = 0.179$	$ \phi _{\max} = 0.0001$ $ \theta _{\max} = 0.0004$ $ \psi _{\max} = 0.0008$ Total ≈ 0.001
Case 4	$ T_{wx} _{\max} = 3.8 \times 10^{-6}$ $ T_{wy} _{\max} = 4.9 \times 10^{-6}$ $ T_{wz} _{\max} = 5.1 \times 10^{-6}$ $T_{w_total} = 1.38 \times 10^{-5}$	$ h_{wx} _{\max} = 0.0666$ $ h_{wy} _{\max} = 0.0996$ $ h_{wz} _{\max} = 0.0129$ $h_{w_total} = 0.179$	$ \phi _{\max} = 0.0001$ $ \theta _{\max} = 0.0004$ $ \psi _{\max} = 0.0005$ Total ≈ 0.001
Case 5	$ T_{wx} _{\max} = 9.6 \times 10^{-7}$ $ T_{wy} _{\max} = 9.2 \times 10^{-6}$ $ T_{wz} _{\max} = 9.2 \times 10^{-5}$ $T_{w_total} = 1.94 \times 10^{-5}$	$ h_{wx} _{\max} = 0.0666$ $ h_{wy} _{\max} = 0.0995$ $ h_{wz} _{\max} = 0.0129$ $h_{w_total} = 0.179$	$ \phi _{\max} = 0.0002$ $ \theta _{\max} = 0.0003$ $ \psi _{\max} = 0.0002$ Total ≈ 0.001
Case 6	$ T_{wx} _{\max} = 3.84 \times 10^{-6}$ $ T_{wy} _{\max} = 3.6 \times 10^{-5}$ $ T_{wz} _{\max} = 1.24 \times 10^{-5}$ $T_{w_total} = 1.99 \times 10^{-5}$	$ h_{wx} _{\max} = 0.0665$ $ h_{wy} _{\max} = 0.0992$ $ h_{wz} _{\max} = 0.0128$ $h_{w_total} = 0.179$	$ \phi _{\max} = 0.0002$ $ \theta _{\max} = 0.0005$ $ \psi _{\max} = 0.0001$ Total ≈ 0.001
Case 7	$ T_{wx} _{\max} = 3.84 \times 10^{-6}$ $ T_{wy} _{\max} = 3.6 \times 10^{-6}$ $ T_{wz} _{\max} = 1.24 \times 10^{-5}$ $T_{w_total} = 1.99 \times 10^{-5}$	$ h_{wx} _{\max} = 0.0665$ $ h_{wy} _{\max} = 0.0992$ $ h_{wz} _{\max} = 0.0128$ $h_{w_total} = 0.179$	$ \phi _{\max} = 0.0002$ $ \theta _{\max} = 0.0005$ $ \psi _{\max} = 0.0001$ Total ≈ 0.001
Case 8	$ T_{wx} _{\max} = 1.7 \times 10^{-6}$ $ T_{wy} _{\max} = 1.0 \times 10^{-5}$ $ T_{wz} _{\max} = 6.7 \times 10^{-6}$ $T_{w_total} = 1.84 \times 10^{-5}$	$ h_{wx} _{\max} = 0.0665$ $ h_{wy} _{\max} = 0.0992$ $ h_{wz} _{\max} = 0.0128$ $h_{w_total} = 0.179$	$ \phi _{\max} = 0.0002$ $ \theta _{\max} = 0.0007$ $ \psi _{\max} = 0.0010$ Total ≈ 0.001

Based on the attitude performances, it can be clearly seen that a full 3-axis attitude control can be achieved in all the cases either using three reaction wheels or four reaction wheels. All performances show that the roll–pitch–yaw attitudes converge to the stable pointing accuracies (≈ 0.001 deg) from the initial attitude errors (± 5 deg) after about 0.035 orbits (197 s), see Figs. 3 and 4. In order to verify the effect of large initial attitude errors, three different initial errors (e.g., 30 deg, -45 deg and 60 deg) are introduced in a test case, i.e., case 1 of the three reaction wheels' configuration. The attitude performances are shown in Fig. 5 confirms that all the attitude errors converge to their steady state (≈ 0.001 deg) at about 197 s. Therefore, the attitude performances given in Figs. 3 and 4 are applicable even in the cases with large initial attitude errors.

4. Summarization

The total control torques, momentums and attitude errors in all the cases are summarized in Tables 3 and 4 corresponding to three and four reaction wheels, respectively. For three reaction wheels, the total minimum torque is in case 5, $T_{w_total} = 1.25 \times 10^{-5}$ Nm, whereby one wheel is aligned along x -axis and the two wheels are tilted; see Fig. 1, case 5. And for four reaction wheels, the total minimum torque is in case 3, $T_{w_total} = 8.57 \times 10^{-6}$ Nm, whereby two wheels are aligned along x - and z -axes and another two wheels are tilted; see Fig. 2, case 3. These minimum torque configurations correspond to the minimum power intake configurations as well. Looking at the pointing performances, all the configurations have a similar total attitude pointing accuracy of about 0.001 deg. Nevertheless, the best attitude pointing (< 0.001 deg) is achieved in case 1 of three reaction wheels. However, this configuration fundamentally inherits a catastrophic failure in the case of one wheel failure compared to all the other configurations; and therefore, it is not a suitable configuration for satellite missions (Sidi, 1997). As the external disturbances are same in all the cases, the total wheel momentum level of about 0.179 N m s is recorded in all the simulations.

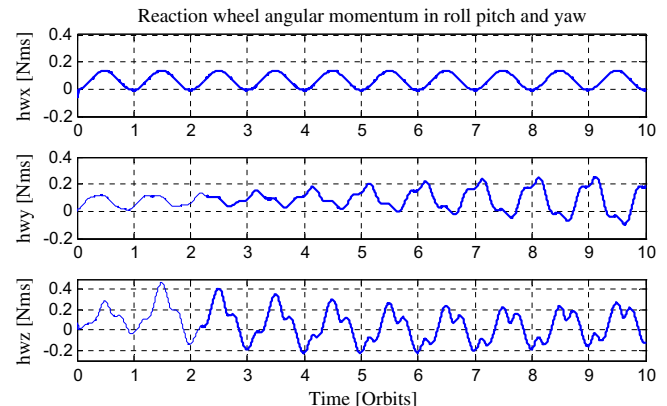


Fig. 6. Reaction wheel angular momentum unloading performances.

5. Wheel angular momentum control performance

Fig. 6 shows an example of the reaction wheel's angular momentum level. The wheel angular momentum control performance shown in Fig. 6 is similar for all the cases. It can be seen that the wheel angular momentum for each axis can be maintained within the suitable limits during the attitude control operation.

6. Conclusion

The satellite attitude control performances using three and four identical reaction wheels have been successfully evaluated in this paper. The results show that a 3-axis satellite attitude control is achieved in all the proposed configurations even with large initial attitude errors. Satellite attitude accuracies around 0.001 deg are achieved in all the configurations with the conventional PD-type (proportional-derivative) controller. In addition, the 3-axis wheel angular momentums are also well maintained during the attitude control task. The total wheel momentum levels in all the configurations are also similar due to the fact that the applied external disturbance torques are identical. Numerical treatments have revealed the reaction wheel configuration with a minimum total torque level. Therefore, the power intake for the attitude control system can be minimized by selecting the minimum torque configuration with respect to a defined reference mission as shown in this work.

References

- Bang, H., Tahk, M.-J., Choi, H.-D. Large angle attitude control of spacecraft with actuator saturation. *Control Eng. Pract.* 11 (9), 989–997, 2003.
- Bayard, D.S. An optimization result with application to optimal spacecraft reaction wheel orientation design. *Proc. Am. Control Conf.* 2, 1473–1478, 2001.
- Beals, G.A., Crum, R.C., Dougherty, H.J., et al. Hubble space telescope precision pointing control system. *J. Guid. Control Dyn.* 11 (2), 119–123, 1988.
- Boyer, F., Alamir, M. Further results on the controllability of a two-wheeled satellite. *J. Guid. Control Dyn.* 30 (2), 611–619, 2007.
- Brief, K., Barwald, W., Gill, E., et al. Technology demonstration by the BIRD-mission. *Acta Astronaut.* 56 (1–2), 57–63, 2005.
- Burns, T.F., Flashner, H. Adaptive control applied to momentum unloading using the low earth orbital environment. *J. Guid. Control Dyn.* 15 (2), 325–333, 1992.
- Camillo, P., Markley, F. Orbit-averaged behavior of magnetic control laws for momentum unloading. *J. Guid. Control Dyn.* 3 (6), 563–568, 1980.
- Chen, Y.H., Hong, Z.C., Lin, C.H. Aerodynamic and gravity gradient stabilization for microsatellites. *Acta Astronaut.* 46 (7), 491–499, 2000.
- Chen, X.-J., Steyn, W.H., Hodgart, S., Hashida, Y. Optimal combined reaction-wheel momentum management for Earth-pointing satellites. *J. Guid. Control Dyn.* 22 (4), 543–550, 1999.
- Ge, X.-S., Chen, L.-Q. Attitude control of a rigid spacecraft with two momentum wheel actuators using genetic algorithm. *Acta Astronaut.* 55 (1), 3–8, 2004.
- Giulietti, F., Quarta, A.A., Tortora, P. Optimal control laws for momentum-wheel desaturation using magnetorquers. *J. Guid. Control Dyn.* 29 (6), 1464–1468, 2006.
- Grassi, M., Pastena, M. Minimum power optimum control of micro-satellite attitude dynamics. *J. Guid. Control Dyn.* 23 (5), 789–804, 2000.
- Hablani, H.B. Sun-tracking commands and reaction wheel sizing with configuration optimization. *J. Guid. Control Dyn.* 17 (4), 805–814, 1994.
- Oh, H.-S., Choi, W.-S., Eun, J.-W. Continuous wheel momentum dumping using magnetic torquers and thrusters. *J. Astronaut. Space Sci.* 13 (2), 194–205, 1996.
- Jin, J., Ko, S., Ryoo, C.-K. Fault tolerant control for satellites with four reaction wheels. *Control Eng. Pract.* 16 (10), 1250–1258, 2008.
- Johnson, C.D., Skelton, R.E. Optimal desaturation of momentum exchange control systems. *AIAA J.* 9 (1), 12–22, 1971.
- Karami, M.A., Sassani, F. Spacecraft momentum dumping using less than three external control torques. *IEEE Syst. Man Cybern.* 4031–4039, 2007.
- Kim, B.J., Lee, H., Choi, S.D. Three-axis reaction wheel attitude control system for KITSAT-3 microsatellite. *Space Technol.* 16 (5–6), 291–296, 1996.
- Krishnan, H., McClamroch, N.H., Reyhanoglu, M. Attitude stabilization of a rigid spacecraft using two momentum wheel actuators. *J. Guid. Control Dyn.* 18 (2), 805–814, 1995.
- Ma, K.B., Zhang, Y., Postrekhin, Y., Chu, W.-K. HTS bearings for space applications: reaction wheel with low power consumption for mini-satellites. *IEEE Trans. Appl. Supercond.* 13 (2), 2275–2278, 2003.
- Nudehi, S.S., Farooq, U., Alasty, A., Issa, J. Satellite attitude control using three reaction wheels. *Proc. Am. Control Conf.*, 4850–4855, 2008.
- Psiaki, M.L. Magnetic torquer attitude control via asymptotic periodic linear quadratic regulation. *J. Guid. Control Dyn.* 24 (2), 386–394, 2001.
- Radford, W.E., Kennedy, L.R.T., Mobley, F. MSX Attitude determination and control hardware. *Johns Hopkins APL Tech. Dig. (Appl. Phys. Lab.)* 17 (2), 153–159, 1996.
- Sidi, M.J. (Ed.). *Spacecraft Dynamics and Control: A Practical Approach*, first ed Cambridge University Press, New York, 1997.
- Silani, E., Lovera, M. Magnetic spacecraft attitude control: a survey and some new results. *Control Eng. Pract.* 13 (3), 357–371, 2005.
- Sinclair, D., Grant, C.C., Zee, R.E. Enabling reaction wheel technology for high performance nanosatellite attitude control, in: *Proceedings of 21st Annual AIAA/USU Conference on Small Satellites*, pp. 1–6, 2007.
- Steyn, W.H. Comparison of low-Earth-orbit satellite attitude controllers submitted to controllability constraints. *J. Guid. Control Dyn.* 17 (4), 795–804, 1994.
- Tavakkoli, A.H., Kabganian, M., Shahravi, M. Modeling of attitude control actuator for a flexible spacecraft using an extended simulation environment, in: *Proceedings of the fifth International Conference on Control and Automation (ICCA'05)*, pp. 147–152, 2005.
- Urukubo, T., Tsuchiya, K., Tsujita, K. Attitude control of a Spacecraft with two reaction wheels. *J. Vib. Control* 10 (9), 1291–1311, 2004.
- Wisniewski, R., Kulczycki, P. Slew maneuver control for spacecraft equipped with star camera and reaction wheels. *Control Eng. Pract.* 13 (3), 349–356, 2005.
- Won, C.-H. Comparative study of various control methods for attitude control of a LEO satellite. *Aerosp. Sci. Technol.* 3 (5), 323–333, 1999.
- Zee, R.E., Matthews, J., Grocott, S.C.O. The MOST microsatellite mission: all systems go for launch, in: *Proceedings of 12th CASI (Canadian Aeronautics and Space Institute) Conferences on Aeronautics*, November, 2002.
- Zhaowei, S., Yunhai, G., Guodong, X., Ping, H. The combined control algorithm for large angle maneuver of HITSAT-1 small satellite. *Acta Astronaut.* 54 (7), 463–469, 2004.